A Study on Key Disciplinary Parameters of Artificial Intelligent-Based Analysis Method for Dynamic Response Prediction of Floating Offshore Wind Turbines

Peng Chen[1]
State Key Laboratory of Ocean Engineering,
Shanghai Jiao Tong University (SJTU),
Shanghai 200240, China;
SJTU-Sanya Yazhou Bay Institute of Deepsea
Science and Technology,
Sanya 572024, China;
Marine, Offshore and Subsea Technology Group,
School of Engineering,
Newcastle University,
Newcastle Upon Tyne NE1 7RU, UK
e-mails: pchen1121@sjtu.edu.cn;
p.chen8@ncl.ac.uk

Zhi Qiang Hu
Marine, Offshore and Subsea Technology Group,
School of Engineering,
Newcastle University,
Newcastle Upon Tyne NE1 7RU, UK
e-mail: zhiqiang.hu@newcastle.ac.uk

The dynamic performance prediction of floating offshore wind turbines (FOWTs) is a challenging task, as the existing theories might not be fully reliable for FOWTs due to the high nonlinearities and coupling effects. The artificial intelligent (AI) method gives a promising solution for this issue, and Chen and Hu proposed a novel AI-based method, named SADA (software-in-the-loop combined artificial intelligence method for dynamic response analysis of FOWTs), to overcome these challenges. This paper addresses a further and in-depth investigation of the key technologies of the key disciplinary parameters (KDPs) in the SADA method to obtain a novel and accurate analysis method for dynamic responses prediction of FOWTs. First, the categorization of KDPs is introduced, which can be divided into three categories: environmental KDPs, disciplinary KDPs, and specific KDPs. Second, two factors, the number of KDPs and boundary adjustment of KDPs, are investigated through the reinforcement learning algorithm within the SADA method. Basin experimental data of a spar-type FOWT is used for AI training. The results show that more proper KDPs set in the SADA method can lead to higher accuracy for the prediction of FOWTs. Besides, reasonable boundary conditions will also contribute to the convergence of the algorithms efficiently. Finally, the instruction on how to better choose KDPs and how to set and adjust their boundary conditions is given in the conclusion. The application of KDPs in the SADA method not only provides a deeper understanding of the dynamic response of the entire FOWTs system but also provides a promising solution to overcome the challenges of validation. [DOI: 10.1115/1.4055993]

Keywords: floating offshore wind turbines, SADA, key disciplinary parameters, reinforcement learning, basin experiment

1 Introduction

The application of floating offshore wind turbines (FOWTs) has great potential, both in terms of economy and sustainability. More demonstration projects and research are being carried out for this very promising industrial application [1]. Many studies for the dynamic response of FOWTs use experimental methods and numerical simulation methods, and there are also successful engineering applications of commercial software and open-source programs in the design or validation of FOWTs [2–6]. However, the design and dynamic performance prediction of FOWTs is still a very challenging task. Currently, there is still a giant gap between reliable numerical tools for FOWTs' dynamic response prediction and the true complicated dynamic responses under complex sea states. For any newly proposed innovative FOWT designs, how to verify its feasibility is still a critical challenge task in terms of numerical analysis tools' credibility, and scale ratio obstacle in traditional basin experiment conduction as well [7].

With the development of artificial intelligent (AI) technology, the data-driven technique has been gradually recognized by academia and industry. The ORCA (Ocean Robotic Asset Certification) Centre, led by Heriot-Watt University and the University of Edinburgh, is pioneering the development of fully autonomous remote services to monitor, maintain, and repair offshore assets such as offshore wind turbines [8]. Garnier et al. [9] and Viquerat et al. [10] gave a general description of the application of deep reinforcement learning (DRL) in fluid mechanics. There have been some promising applications of introducing machine learning techniques in the offshore renewable energy field. Li et al. [11,12] studied the wave energy control algorithm with an artificial neural network (ANN) to implement the real-time wave force prediction. Xie et al. [13] applied DRL to the control system of the breakwater to find the best strategy for wave dissipation.

In general, the application of machine learning in the field of traditional wind energy is relatively mature and widely recognized by the scientific community. However, most of the existing applications are based on land-based wind turbines for wind energy harvesting devices. Li and Shi [14] used three ANNs to forecast wind speed, which is critical for wind energy conversion systems. Further research has been done by Pelletier et al. [15] who used ANN to obtain the power curves of the wind turbine with six parameters. Li [16] discussed the temporal characteristic of wind power

[1]Corresponding author.

Contributed by the Ocean, Offshore, and Arctic Engineering Division of ASME for publication in the Journal of Offshore Mechanics and Arctic Engineering. Manuscript received March 12, 2022; final manuscript received October 4, 2022; published online November 17, 2022. Assoc. Editor: Qing Xiao.

generation. The recurrent multilayer perceptron neural network is trained based on the time algorithm of the extended Kalman filter to predict the power of the wind turbine. Kusiak et al. [17] used weather forecast data generated in different time scales and ranges to establish short-term and long-term prediction models for wind farm power. And they also verified that the model generated by the neural network is superior to other models in both short-term and long-term prediction. The wake effect is also a major and complex issue in the wind power industry. Sun et al. [18] proposed a power prediction model based on an artificial neural network and optimized the yaw angle to minimize the impact on the overall wake of the wind turbine. The model can estimate the total power generation of a wind turbine for a given wind speed, wind direction, and yaw angle. Stetco et al. [19] conducted a systematic review of conditions for monitoring in 2019. For example, blade failure detection or generator temperature monitoring. At the same time, they classified the Machine Learning model including data source, feature selection, and extraction, model selection (classification and regression), verification, and decision-making. Among them, neural networks, support vector machines, and decision trees are mostly used.

However, how understanding the phenomenon more deeply and promoting the further development of AI-based technology in FOWTs' design, manufacture, installation, and maintenance, is the focal concern of the wind industry and academic community. Therefore, the combination of fundamental theories, numerical tools, and AI technology is the trend for the development of FOWTs. Based on the previous research outcomes, an innovative AI-based method, named SADA, was newly proposed by Chen et al. [20]. The full name of SADA is "**S**oftware-in-the-Loop combined **A**rtificial Intelligence Method for **D**ynamic Response **A**nalysis of FOWTs." It combines the AI technology into an in-house numerical program *DARwind* (dynamic analysis for the response of wind turbines) to analyze and predict dynamic responses of FOWTs. Through the SADA method, the program *DARwind* is trained to be intelligent for the objective FOWT, using the AI training process with basin experimental data or onsite full-scale measurement data. SADA method cannot only bring more accurate predictions on dynamic responses of FOWTs but also provide an alternative way to dig the in-depth knowledge involved in FOWTs.

In the application of the SADA method, the first and one of the most critical steps is the inclusion of key discipline parameters (KDPs). The proposal of KDPs is of great importance for a reasonable application of the SADA method. It is the data transfer interface between AI technology and FOWTs design and application. Many theories involved in FOWTs' dynamic models include massive functions and formulas which are conventionally determined based on assumptions and empirical parameter values. However, many assumptions and empirical parameters were not initially proposed for FOWTs but inherited from land-based wind turbines, traditional floating offshore units, or other engineering applications. For example, the lift or drag coefficient of wind turbine blades in aerodynamics can bring potential problems. Many other key environmental parameters such as viscous damping in hydrodynamics, mooring line damping values, etc. are also difficult to be issued unique values during the analysis [20]. These parameters belong to the category of KDPs, which will be discussed in this paper.

How to analyze and optimize these KDPs through the existing design technology is very lacking in the current FOWTs research. On the one hand, these KDPs cover a wide range of disciplines. On the other hand, it is difficult to carry out traditional research methods on these KDPs under the nonlinear coupling conditions of FOWTs. It is undeniable that these KDPs are critical to the dynamic response of the entire FOWTs in traditional theory revision and innovation verification. The SADA method provides a possibility for in-depth analysis of these KDPs in terms of the quantity or the quantitative study of each KDP. Therefore, the study in this paper aims to answer four main issues regarding the concept of KDPs in the SADA method, which are:

- What physical quantities are included in KDPs in the field of FOWTs?
- What is the influence of different numbers of KDPs affecting the dynamic response of FOWTs?
- What is the influence of boundary conditions (BCs) of KDPs affecting the dynamic response of FOWTs?
- How to adjust the boundary conditions of KDPs in response to some specific situations?

Therefore, the different classifications of KDPs in SADA will be introduced. And then, the impact of KDPs change on the dynamic response of the FOWTs system is analyzed on platform motions, thrust or fairlead tensions, etc. from different quantities and boundary conditions. Finally, a guideline for the selection of KDPs and the definition of boundary conditions is proposed to conduct further research by the SADA method. In summary, this study not only provides more feasibility for the analysis of KDPs involved in FOWTs but also provides more reliable reference information for the design and verification of FOWTs through in-depth research on these KDPs. In addition, it can also help other designers and scholars to gain a deeper understanding of these KDPs through the guidelines.

2 A Brief Description of the SADA Method

This section gives a brief description of the SADA method including the KDPs concepts, *DARwind* program, an AI algorithm, and more details can be referred to Refs. [20,21].

SADA is a novel concept to integrate the AI technology (artificial neural networks and deep reinforcement learning) and *DARwind* (a coupled aero-hydro-servo-elastic program) for optimized design and dynamic performance prediction of FOWTs. Figure 1 shows the general flowchart of the entire SADA algorithm. First, the concept of key disciplinary parameters (KDPs) is proposed, and it is the most crucial concept in SADA, working as a data transmission interface between AI technology and disciplines in numerical simulation of FOWTs. Specifically, the KDPs can be divided into three categories (environmental KDPs, disciplinary KDPs, and specific KDPs), with their unique boundary conditions in SADA. Second, *DARwind* can be trained to be more intelligent and give more accurate predictions for FOWTs by ANN or DRL algorithms on target data (experimental or full-scale measured data). All information generated in the iterative loop will be recorded, including the change of KDPs and the corresponding percentage difference of FOWTs simulation.

2.1 Key Disciplinary Parameters. It is challenging to obtain accurate forecasts and develop an integrated design by measurement, experiments (basin or wind tunnels), and numerical simulation. The disciplinary knowledge involved in FOWTs is very complex and has strong nonlinearity. Therefore, KDPs are proposed in SADA as a concept covering multiple disciplines and aspects, including various uncertain or experience-based parameters.

In SADA, KDPs interface traditional numerical computation and neural network parameter optimization, which can be adjusted based on the percentage difference evaluation with the specific target data and the weighting of the deep neural network. However, the corresponding boundary condition would limit each KDP. More information on KDPs can be found in Sec. 3. The flowchart of KDPs selection is shown in Fig. 2. The specific decision process is as follows:

- Step 1: Choose the corresponding KDPs in three categories.
- Step 2: Use the concept of significant figures to set the boundary conditions according to the specific values of each KDP.
- Step 3: Determine the percentage difference between the numerical results and the target data.
- Step 4: Adjust the boundary conditions appropriately.

2.2 DARwind. FOWTs bear complex sea environmental loads, including waves, the current, wind, etc. In addition to

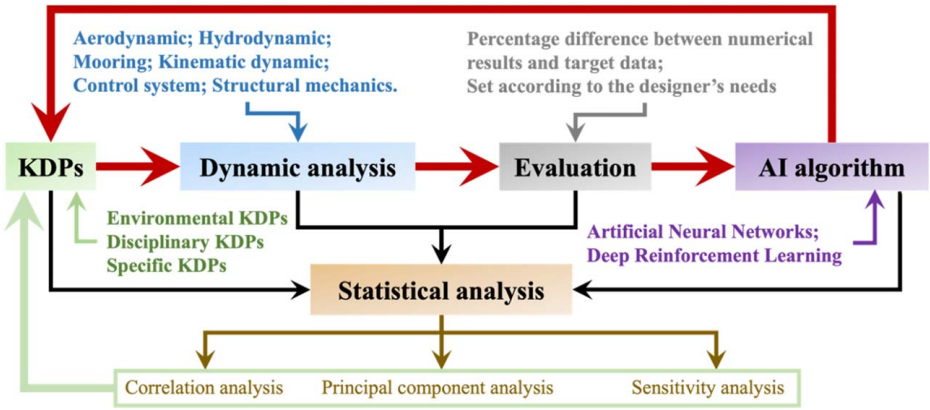

Fig. 1 General flowchart of the SADA method

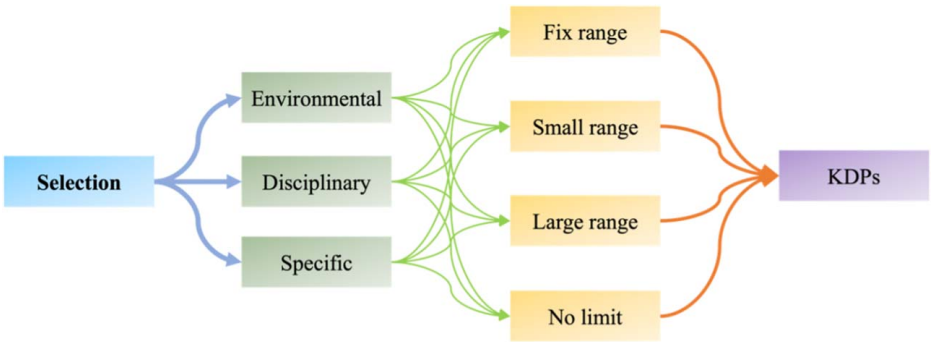

Fig. 2 KDPs selection flowchart

mooring systems and control systems, these are usually decoupled from the main structure and calculated as external forces in the numerical calculation. Therefore, a fully coupled aero-hydro-servo-elastic method was developed and then programed as an integrated code *DARwind* (dynamic analysis for response of wind turbines) to simulate the dynamic response of FOWTs. The current version of *DARwind* is written in the high-level programming language FORTRAN, verified by a series of code-to-experiment comparisons to show its feasibility. The functional modules of the *DARwind* program can be roughly divided into the input module, solver module, and output module, as shown in Fig. 3. In addition, the relevant theoretical method used is shown in Fig. 4; for more specific information and validation of *DARwind*, please refer to Ref. [22].

2.3 Artificial Intelligent Application. In this section, the application of DRL in SADA is introduced, mainly feature engineering and reward engineering. Furthermore, the DRL module's two algorithms in SADA are the Brute-force algorithm and the deep reinforcement learning algorithm.

2.3.1 Notations. The development of DRL is rapid, but its mathematical principles are very complex, far more than deep learning. The most successful applications are basically in Atari, Go, and other games. In summary, the application of DRL in SADA is the most innovative highlight. The specific notations and nouns combined FOWTs and DRL in SADA can be seen in Fig. 5.

The main body of DRL is called an agent, which often makes decisions or actions. For example, vehicles are agents in the application of automatic driving. Correspondingly in SADA, *DARwind* will adjust the KDPs and conduct a dynamic response analysis of FOWTs, so *DARwind* is an agent. The environment is what the agent interacts with, which can be abstractly understood as the rules or mechanisms in the interaction process. In automatic driving applications, the actual physical world is the environment. In the same way, it is the actual environment of FOWTs.

The state is not unique, and it can be the feedback of the environment or the feedback of the agent. In the example of autonomous driving, the analysis of road conditions and the state of the car (vehicle speed, fuel consumption, etc.) can be considered states. In the SADA method, the dynamic responses of FOWTs can be considered as states. The observation of the environment can be real-time or partial. For example, vehicle speed and changes in road conditions need to be observed in real-time.

Actions are decisions made by the agent based on the current state. The selection of actions can be deterministic or random. Random refers to the selection of actions with a certain probability. Action space is the set of all possible actions, denoted A. It can be discrete, continuous, finite, or infinite sets. There are many actions to control the car in autonomous driving, including braking, accelerator, steering wheel, indicator lights, etc. These actions include discrete actions (playing the indicator light) and continuous actions (playing the steering wheel). In SADA, the actions are adjustments to KDPs. Since the values of KDPs belong to a continuous distribution, the action space in SADA belongs to a continuous infinite set.

2.3.2 Feature Engineering. As an agent, *DARwind* will take continuous action through the software-in-the-loop (SIL) algorithm, i.e., adjusting KDPs appropriately to obtain more accurate prediction results and minimize the percentage difference in the dynamic performance of FOWTs. The action here affects the immediate reward and the next state, thus the subsequent reward. The purpose of *DARwind* is to find what action can be taken to maximize the numerical reward signal. The roles of the deep neural networks are amplified to record (state, action, reward, next state) in different situations through the SIL algorithm. In this paper, the SADA algorithm is mainly based on the statistical index of the average value.

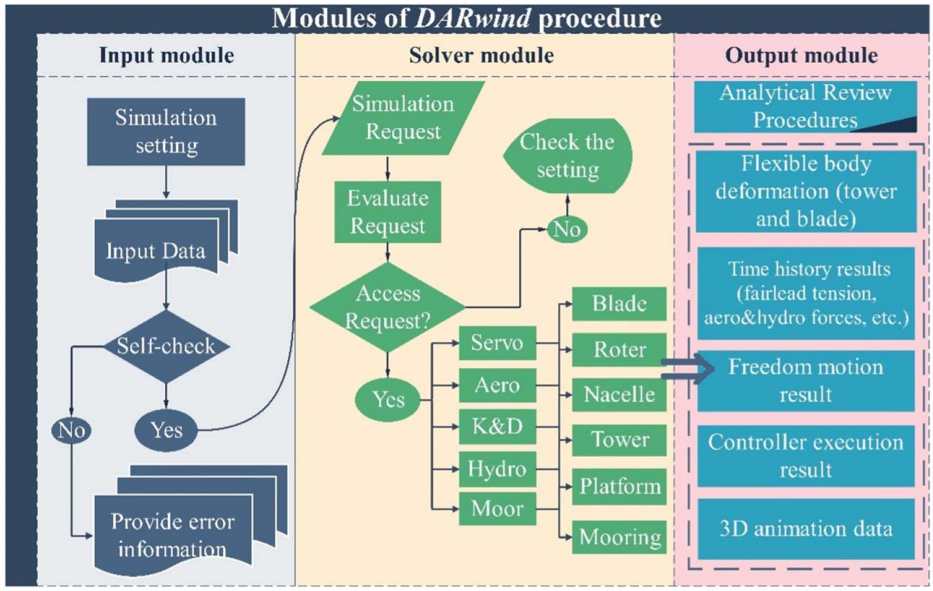

Fig. 3 Modules of *DARwind* procedure

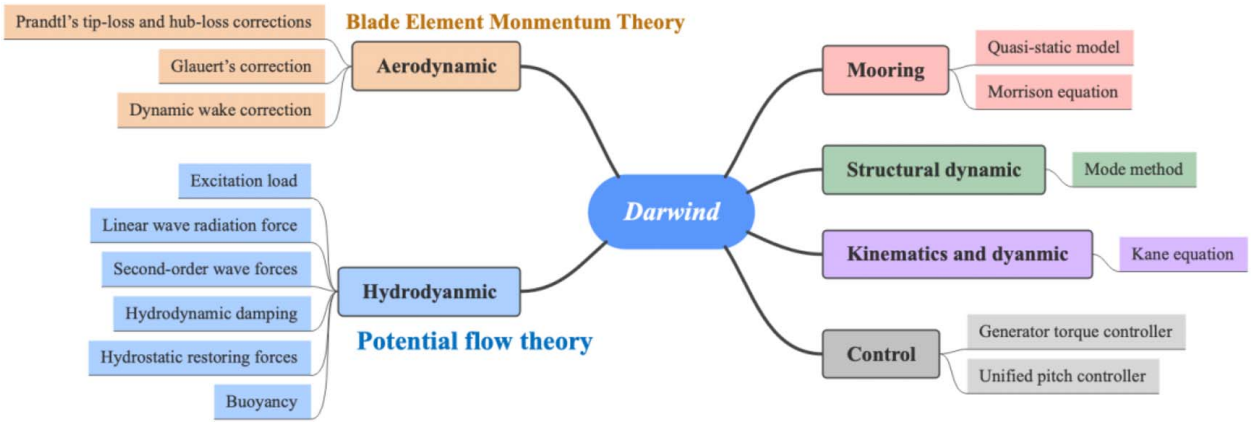

Fig. 4 Theoretical method of *DARwind* modules

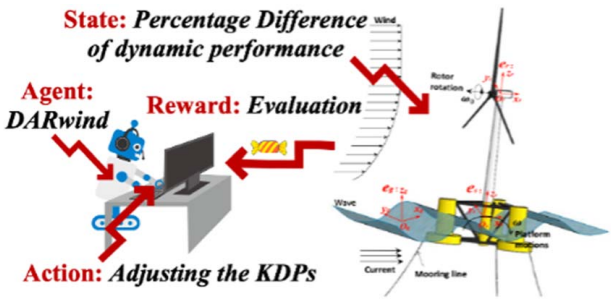

Fig. 5 RL notations in SADA

The reward here is the feedback on the evaluation of percentage differences, which are

$$\begin{cases} P_{\text{initial}} = \left| \dfrac{O_{\text{target data}} - O_{\text{initial KDPs}}}{O_{\text{target data}}} \right| \times 100\% \\ P_{\text{present}} = \left| \dfrac{O_{\text{target data}} - O_{\text{weighted KDPs}}}{O_{\text{target data}}} \right| \times 100\% \\ P_{\text{difference}} = P_{\text{initial}} - P_{\text{present}} \end{cases} \tag{1}$$

The $O_{\text{target data}}$ is the target data which can be the experimental results or measured data. The $O_{\text{initial KDPs}}$ is the numerical results by initial KDPs. $O_{\text{weighted KDPs}}$ is the numerical results by weighted KDPs. The $P_{\text{difference}}$ are used to measure whether the results of SADA are better than the initial KDPs. If the $P_{\text{difference}}$ is positive, it means that the difference between target data and numerical results has decreased by SADA, otherwise the difference has increased. In short, evaluation of $P_{\text{difference}}$ is to establish a reward mechanism to tell *DARwind* how much benefit has been obtained in this iteration. The main consideration in this paper is the mean value of time history data.

In addition to the $P_{\text{difference}}$ evaluation in feature engineering and reward engineering, target data are not the only criterion. One of the challenges of setting reward engineering in SADA is that the *DARwind* needs to learn, approach actions, and finally, achieve the goal that the designer hopes. If the designer's goal is easy to distinguish, this task may be solved well, such as finding the most minor $P_{\text{difference}}$ of a physical quantity or balancing the $P_{\text{difference}}$ among multiple physical quantities. Nevertheless, in some problems, the designer's goal is challenging to quantify, and it is not easy to be translated into a loss function, especially when these problems require the agent to make very skillful actions to complete complex tasks or a series of tasks.

2.3.3 Reward Engineering. In practice, a reasonable result signal can make the agent learn successfully and efficiently and can effectively feedback and guide the agent to learn during the

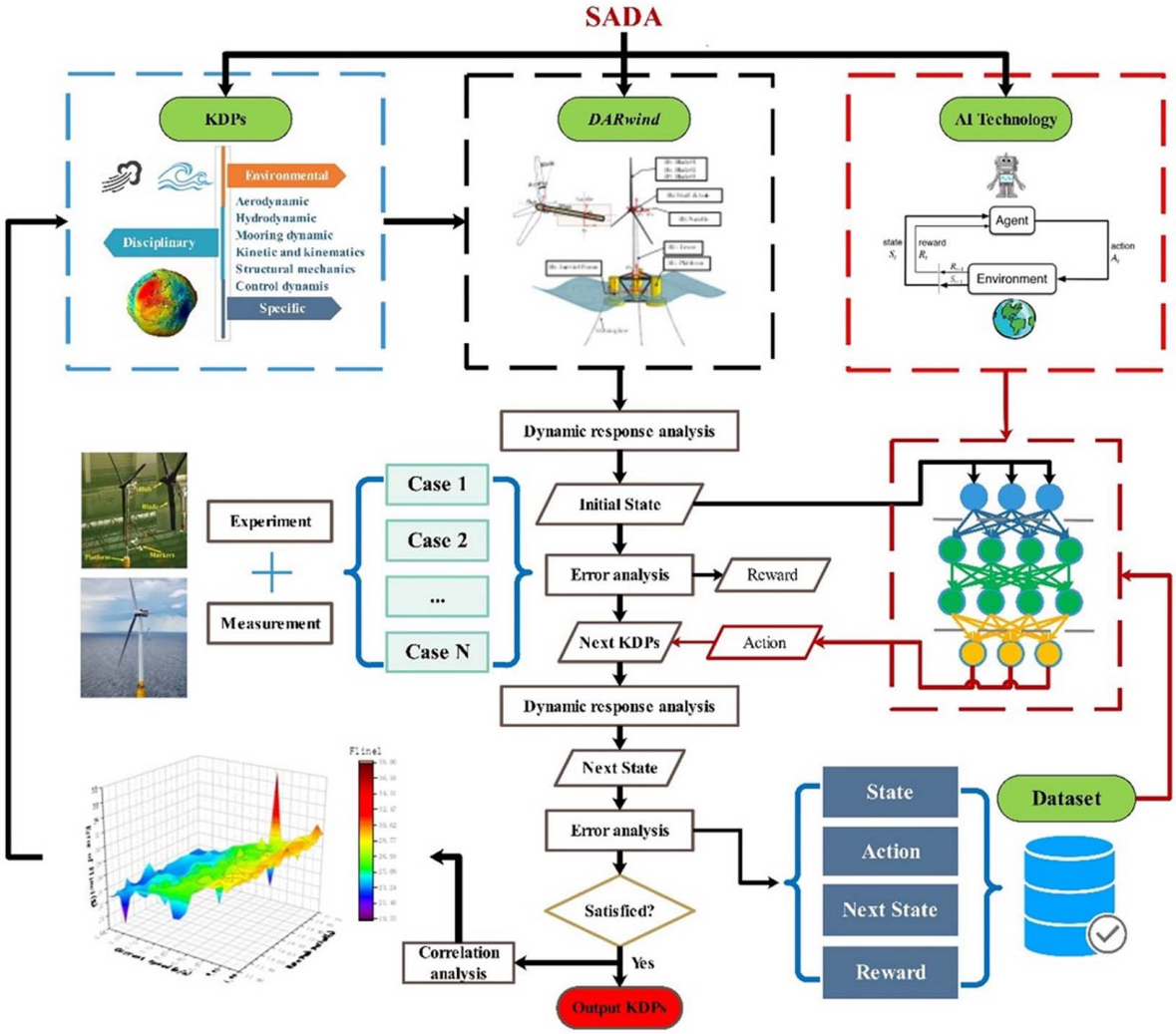

Fig. 6 The layout of SADA

process of interacting with the environment. For SADA, reward engineering is not unique. For example, when the surge and pitch are used as the target physical quantities, the reward project is based on the $P_{\text{difference}}$ of these two physical quantities. The change in the $P_{\text{difference}}$ reflects the feedback on the quality of the action. In addition to the profit target of $P_{\text{difference}}$, the $P_{\text{difference}}$ continuity of each iteration will also be randomly selected in the reward engineering.

In summary, as shown in Fig. 6, SADA starts by selecting the initial critical KDPs by FOWT designers. Then, some physical quantities such as 6DOF platform motions are chosen as the states in the DRL algorithm. According to the states, the agent will give the corresponding action to adjust the KDPs values properly to run the next loop if the evaluation is not satisfied. When the percentage difference is reduced to an acceptable range, this means that the program is good enough to conduct the final numerical analysis. In addition, some other physical quantities that cannot be measured directly in the experiment or measurement can be predicted as well. Such as the deformation of the blade and tower. Besides, SADA can also exclusively complete the FOWTs dynamic response analysis in the sea states different from those used in basin experiments or measurement through the training process.

3 Key Discipline Parameters in FOWTs

This section will introduce the concept of KDPs with some examples in terms of environmental KDPs, disciplinary KDPs, and specific KDPs. In general, the category of KDPs can be shown in Fig. 7.

3.1 Environmental Key Disciplinary Parameters. In the most current numerical simulation for dynamic analysis of FOWTs, a wide range of parameters rely on empirical data and require manual input. These parameters vary with different models and locations, such as gravitational acceleration, water density, air viscosity, operational water depth, etc.

First, air density can be taken as an example. With the difference in altitude, temperature, and air pressure in various regions, the air density is also different. Under different air pressure, temperature, and water vapor pressure, the calculation formula of air density can be defined as

$$\rho = \frac{1.276}{1 + 0.00366t} \times \frac{p - 0.38e}{1000} \tag{2}$$

where p is the pressure, t is the temperature, and e is the water vapor pressure. The sea level for a wind turbine is relatively high. For example, 5 MW FOWT Hywind has a tower height of 77.6 m and a blade length of 63 m. This means that the size-changing of blades or tower height and wake effect will vary air density and viscosity. It will impact the wind load applied to the rotating blades, though these effects have been mostly neglected in the current numerical program. The empirical formula for calculating air

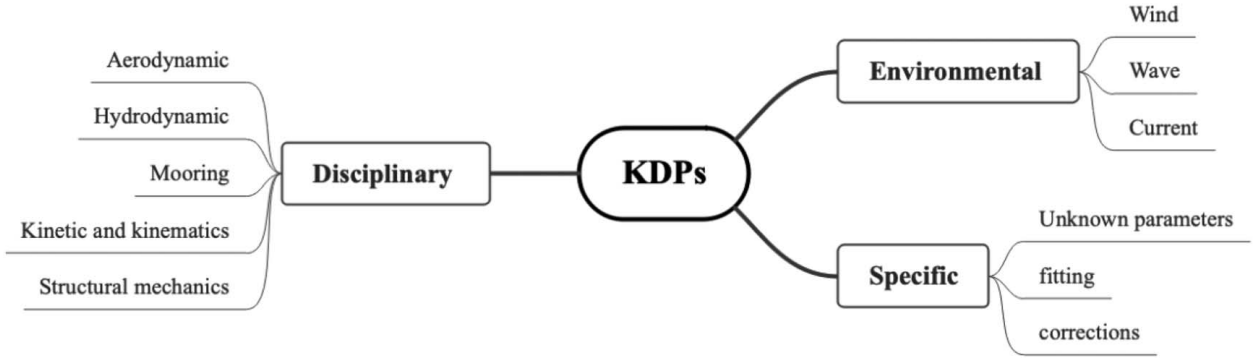

Fig. 7 The category of KDPs

density changes with altitude is

$$\rho = 1.225e^{-0.0001h} \tag{3}$$

where ρ is the air density corresponding to height h. Therefore, in this example, the empirical value of -0.0001 before h can be considered a KDP. The value of this parameter can be changed within a range in the SADA method to consider the variation of air density.

Second, considering the viscous effect of sea level on wind speed, the change of the average wind speed gradient along the height conforms to the logarithmic rate:

$$\bar{u}(z) = \bar{u}(h)\left(\frac{z}{h}\right)^{1/n} \tag{4}$$

where h is the reference height above sea level and is usually 10 m; $\bar{u}(h)$ is the average wind speed at the reference height; z is above sea level; $\bar{u}(z)$ is the average wind speed at z; and n is the wind profile index, which characterizes the sea level roughness. For the open coastal area, the value of n is usually 3; for the uncovered sea area, the value is usually 7–8. But its real value varies and depends on quite a lot of experience in simulation, so parameter n is chosen as one KDP.

Third, for wave load calculation, the Joint North Sea Wave Project (JONSWAP) type spectrum is popularly used to simulate the irregular waves in FOWT analysis. The 17th International Towing Tank Conference (ITTC) recommended the following JONSWAP type spectrum for limited fetch [23]:

$$S(\omega) = 155\frac{H_{1/3}^2}{T_1^4\omega^5}\exp\left(\frac{-944}{T_1^4\omega^4}\right)3.3^{\exp\left[-\left((0.191\omega T_1-1)/\sqrt{2}\sigma\right)^2\right]} \tag{5}$$

where

$$\sigma = \begin{cases} 0.07 & \text{for } \omega \le 5.24/T_p \\ 0.09 & \text{for } \omega > 5.24/T_p \end{cases}$$

$H_{1/3}$ is the significant wave height defined as the mean of the one-third highest waves and T_1 is a mean wave period. In the JONSWAP spectrum, their value can be adjusted in the SADA method during the AI optimization process. Similarly, the peak period and the wave direction can all be selected as KDPs in the SADA method.

Fourth, the parameters of current also can be selected as KDPs. The current model in numerical analysis can be expressed as follows:

$$U_C(z) = U_0\left(\frac{z+h}{h}\right)^c \tag{6}$$

where z is the vertical depth below the water surface; h is the depth of the water to the bottom; and U_0 is the water velocity at the free surface. Parameter c commonly uses empirical value 1/7, but it varies for different sea states. Thus, c and U_0 can be chosen as the environmental KDPs.

In general, the above-mentioned environmental KDPs, especially wind and waves, have a significant impact on the dynamic response of the FOWTs system. A slight difference may significantly change the entire system's dynamic response because the FOWT is a high nonlinear coupling system, and all the disciplines involved are highly coupled to others. This characteristic makes the application of AI technology in the analysis essential.

3.2 Disciplinary Key Disciplinary Parameters. Disciplinary KDPs constitute the largest category of KDPs. Those empirical formulas and parameter values in the fundamental theories for calculating loads, motions, and all the dynamic responses of FOWTs can be put in the disciplinary KDPs category. Many of the empirical formulas and parameters involved in physical modeling are determined based on assumptions or practical fitting works. Some assumptions and empirical parameters are not explicitly designed for FOWTs but are inherited from land-based wind turbines and offshore oil and gas engineering practices. Therefore, many KDPs can be defined in this category. The following will use KDPs in aerodynamics, and hydrodynamics as examples to introduce the disciplinary KDPs.

3.2.1 Aerodynamic Parameters of Key Disciplinary Parameters. Aerodynamic load is one of the dominating loads applied on FOWTs. Conventional aerodynamics theories include one-dimensional momentum theory (ideal disk) and 2D blade element momentum theory (BEMT) for the simulation and experimental design. But there are many assumptions and empirical parameters popularly used in these theories. For the BEMT model, there are some critical assumptions, such as no radial dependency. Many correction models also use empirical parameter values, such as *Prandtl's* tip loss factor and *Glauert* correction parameters.

For aerodynamic calculation, when the axial induction factor becomes more significant than approximately 0.4, the simple momentum theory breaks down. Different empirical relations between the thrust coefficient C_T and a can be made to fit with measurements, for example:

$$C_T = \begin{cases} 4a(1-a)F, & a \le a_c \\ 4a\left(1-\frac{1}{4}(5-3a)a\right)F, & a > a_c \end{cases} \tag{7}$$

F is Prandtl's tip loss factor and corrects the assumption of an infinite number of blades. For details refer to Eq. (6.38) in Ref. [24] and a_c is approximately 0.2. Because a_c is an empirical value, so it is chosen as one KDP.

Take Prandtl's tip loss factor as an example. For a rotor with a finite number of blades, the vortex system in the wake is different from a rotor with an infinite number of blades. The relevant formula is as follows:

$$\begin{cases} F_P = \frac{2}{\pi}\arcsin(e^{-f}) \\ f = \frac{N(R-r)}{2r\sin\varphi} \end{cases} \tag{8}$$

where N is the number of blades, R is the total radius of the rotor, r is the local radius of the blade element, and φ is the flow angle. In some cases, when f is less than 7, it can be calculated according to the F_P parameter. When f is greater than 7, the change is small so that the tip loss can be neglected. Therefore, the threshold value 7 plays an essential role in the aerodynamic load calculation. However, this threshold value was initially proposed and determined based on onshore wind turbine theories. For FOWTs, this threshold value could be different, and therefore it can be defined as a disciplinary KDP.

3.2.2 Hydrodynamic Parameters of Key Disciplinary Parameters. Potential flow theory and Morison's equation are commonly used methods for hydrodynamic load calculation in FOWT analysis. Nevertheless, the potential flow damping cannot consider the viscous effect of fluids accurately.

As for FOWTs, when the supporting platform is a Spar-type floater, the calculation of viscous damping force can use Morrison's equation:

$$d\boldsymbol{F}_{\boldsymbol{m}}^{\boldsymbol{V}} = -\frac{\rho}{2} C_D^M D dz \cdot (\boldsymbol{v}_{\boldsymbol{w}} - \boldsymbol{v}_{\boldsymbol{s}}) \cdot |\boldsymbol{v}_{\boldsymbol{w}} - \boldsymbol{v}_{\boldsymbol{s}}| \tag{9}$$

where D is the diameter of the cylinder; $\boldsymbol{v}_{\boldsymbol{w}}$ and $\boldsymbol{v}_{\boldsymbol{s}}$ are the wave and structure velocities, respectively; and C_D^M is the drag coefficient. Among these parameters, drag coefficient and added mass coefficient both have empirical values and are quite crucial for the hydrodynamic load calculation. So, the drag coefficient and added mass coefficient can also be selected as disciplinary KDPs.

In the static water flow field, the FOWTs will also change the wet surface due to the motions of the floating body, which will cause the static water pressure to change and be affected by the restoring force of the static water.

$$F^S = \begin{bmatrix} 0 & 0 & \rho g V_\nabla & 0 & 0 & 0 \end{bmatrix}^T - \boldsymbol{C} \cdot \boldsymbol{X} \tag{10}$$

$$\boldsymbol{C} = \begin{bmatrix} 0 & 0 & 0 & 0 & 0 & 0 \\ 0 & 0 & 0 & 0 & 0 & 0 \\ 0 & 0 & \rho g A_w & 0 & 0 & 0 \\ 0 & 0 & 0 & \rho g (I_x + z_B V_\nabla) & 0 & 0 \\ 0 & 0 & 0 & 0 & \rho g (I_y + z_B V_\nabla) & 0 \\ 0 & 0 & 0 & 0 & 0 & 0 \end{bmatrix} \tag{11}$$

The restoring force also needs to be compared with the experimental results in the numerical calculation. The parameters in the added restoring force matrix are very significant KDPs.

3.3 Specific Key Disciplinary Parameters. For specific KDPs, some experimental models or design parameters of the full-scale FOWTs are different from the actual physical models. In addition, due to commercial confidentiality, it is impossible to obtain all the design parameters. For FOWTs, there are many new physical phenomena worth exploring, and if these phenomena involve an additional force, moment, and damping, they can also be considered in specific KDPs.

Besides, some experiments used static lines or cables to replace a static thrust from a given turbine's thrust curve or drag discs to reproduce the static wind loading. There is also the simplification of the mooring lines model: use the quasi-static catenary equation to replace the delta link of multi-lines by increasing the yaw stiffness. As for potential flow theory, there are also some empirical parameters based on previous experiments. Their values might not be accurate for FOWT calculation, and these empirical parameters involved can be classified as specific KDPs.

3.4 Boundary Conditions of Key Disciplinary Parameters. To adjust KDPs efficiently in the SADA method, the boundary conditions of the KDPs must be adequately defined. This section will discuss the boundary conditions of KDPs. Figure 8 shows the flowchart of KDP and boundary conditions in SADA.

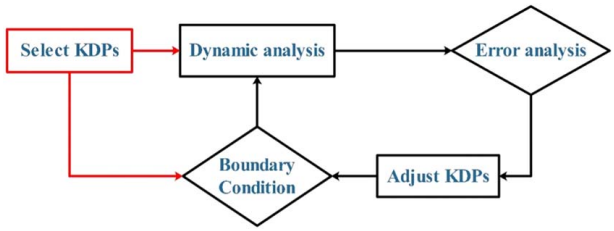

Fig. 8 The flowchart of KDP and boundary conditions

A good boundary condition can speed up the convergence of SADA and reflect the rationality of the dynamic response of FOWTs accurately. Each KDP has a specific value, and the magnitude of their values may vary quite a lot, so the boundary conditions are also set on this basis. Although the amplitude of each KDP is different, the significant figures of these KDPs values can also provide a reliable classification and setting method.

Therefore, based on significant figures of each KDP, the general formula for defining their boundary conditions can be defined as

$$\begin{cases} X \in [X - a \cdot 10^{(-X_{\mathrm{SF}})},\ X + a \cdot 10^{(-X_{\mathrm{SF}})}], & 0 \le |X| \le 1 \\ X \in [X - a \cdot 10^{(Y - X_{\mathrm{SF}})},\ X + a \cdot 10^{(Y - X_{\mathrm{SF}})}], & 1 < |X| \le 10 \\ X \in [X - a \cdot 10^{(Y-2)},\ X + a \cdot 10^{(Y-2)}], & |X| > 10 \end{cases} \tag{12}$$

where X is the value of KDPs; Y is the number of digits to the left of the decimal point; X_{SF} is the significant figures of the KDPs value; and a is the boundary condition coefficient, which determines the range of the boundary conditions of KDPs. The three specific ranges in Eq. (12) are shown in the following formulas:

$$\mathrm{BC} = \begin{cases} \text{Fix range} & a = 0 \\ \text{Small range} & a \in [-1,\ 1] \\ \text{Large range} & a \in [-5,\ 5] \\ \text{No range limit} & |a| > 5 \end{cases} \tag{13}$$

To better understand the definitions of Eqs. (12) and (13), take wind speed V_{wind}^A in aerodynamics and viscous damping coefficient $C_{\mathrm{VD}(1,1)}^H$ and current speed V_{current}^H in hydrodynamics as examples to demonstrate how to use Eqs. (12) and (13) to choose the corresponding boundary conditions.

As for the steady wind speed in aerodynamics, if $V_{\mathrm{wind}}^A = 9.5\ \mathrm{m/s}$, then $Y = 1$ and $X_{\mathrm{SF}} = 2$, so the three boundary conditions are

$$V_{\mathrm{wind}}^A(\mathrm{BC}) = \begin{cases} \text{Small range} \in [9.49,\ 9.51], & a = 0.1 \\ \text{Large range} \in [9,\ 10], & a = 5 \\ \text{No range limit} \in [0,\ 19.5], & a = 100 \end{cases}$$

In the boundary condition without range limitation, the value of a is 15. The original boundary condition should be [−0.5, 19.5]. The steady wind speed cannot be negative, so the default here is [0, 19.5].

As for the added viscous damping coefficient in hydrodynamics, if $C_{\mathrm{VD}(1,1)}^H = 10,000.0$, then $Y = 5$, so the three boundary conditions are

$$C_{\mathrm{VD}(1,1)}^H(\mathrm{BC}) = \begin{cases} \text{Small ange} \in [9000,\ 11,000], & a = 1 \\ \text{Large range} \in [5000,\ 15,000], & a = 5 \\ \text{No range limit} \in [-1000,\ 21,000], & a = 11 \end{cases}$$

Similar to current speed, if $V_{\mathrm{current}}^H = 0.05\ \mathrm{m/s}$, then $X_{\mathrm{SF}} = 3$, so the three boundary conditions are

$$V_{\mathrm{current}}^H(\mathrm{BC}) = \begin{cases} \text{Small range} \in [0.049,\ 0.051], & a = 1 \\ \text{Large range} \in [0.045,\ 0.055], & a = 5 \\ \text{No range limit} \in [0,\ 0.1], & a = 50 \end{cases}$$

The above discussion and classification of KDPs boundary conditions are only for general situations. For some specific KDPs, the actual boundary conditions must be combined to make judgments based on their value of them.

4 Case Study for Key Disciplinary Parameters

In this section, a case study for the application of KDPs in the SADA method is presented. It is aimed to show that the KDPs can be selected and what are the roles of KDPs in the process of the SADA method. In addition, it is also aimed to demonstrate the advantage of the SADA method with this case study. This section starts with a case set, a brief introduction of the analysis case; and then a detailed explanation of KDPs selection is given. The numbers and boundary conditions of KDPs in the case study are shown to further discuss how to better choose more effective KDPs and how to define their boundary conditions.

4.1 Case Setting. In this section, a case setting and KDPs in this paper are introduced. The case study is proposed from the results of a basin experiment of FOWTs. It is a basin experiment conducted at Deepwater Offshore Basin at Shanghai Jiao Tong University with a model setup corresponding to a 1:50 Froude scaling. Figure 9 shows the experimental model of the 5 MW Spar-type FOWT. More details can be found in Ref. [25]. Table 1 shows the experimental case used for the case study analysis.

4.2 Key Disciplinary Parameters Selection and Boundary Condition Setting. This section introduces a basic process of the selection of KDPs for analysis in terms of number and category. In addition, the specific boundary conditions are grouped and sorted for these KDPs.

4.2.1 Thirty-Nine Selected Key Disciplinary Parameters. First, the KDPs involved in this article are introduced. According to the three types of KDPs discussed above, 39 of KDPs are selected as the basis for the analysis. Table 2 shows the selected KDPs. Among them, categories A, B, and C are the categories of environmental KDPs, disciplinary KDPs, and specific KDPs, respectively. For some KDPs, they will be subdivided into multiple values. For example, due to the symmetry of the floating body, only the diagonal parameters of the added viscous damping coefficient matrix and the added restoring force coefficient matrix are considered hydrodynamic disciplinary KDPs. Therefore, there will be six KDPs in added linear viscous damping matrix.

4.2.2 Grouping for Quantitative Analysis. To better study the impact of different numbers and types of KDPs on the dynamic response of the FOWTs system, 39 KDPs are divided into three groups. In the first group, environmental KDPs for wind, wave, and current are included. In the second group, the environmental KDPs and disciplinary KDPs are included. In the third group, all 39 KDPs are considered:

- Group 1: A (5 KDPs)
- Group 2: A + B (20 KDPs)
- Group 3: A + B + C (39KDPs)

For the establishment of three groups, the optimization effect of SADA including different types and numbers of KDPs can be compared.

4.2.3 Grouping for Boundary Condition Analysis. The study of BCs for KDPs is also important, and it is grouped based on the range definitions in Sec. 4.

(a) Fix (no range)
(b) Small range
(c) Large range
(d) No limit range

A total of 39 KDPs are divided into three categories (A, B, and C), and four sets of BCs are used to permutate and combine to obtain eight sets of BCs in Table 3. This can maximize the impact of different types of KDPs and the effects of their boundary conditions for analysis. Taking the BC1 as an example, only A (environmental KDPs) allows small changes, and B (disciplinary KDPs) and C (specific KDPs) remain unchanged in SADA calculation. The difference between BC3 and BC4 is that the KDPs of the environment have larger variations. The difference between BC6 and BC7 is that the variations of environmental KDPs are not limited. Through this grouping method, not only can the influence of different types of KDPs on the dynamic response of the FOWTs system be analyzed but also the optimization effect comparison under different BCs can also be obtained.

Table 1 Case matrix

	Wind speed, V_w	Wave height, H_s	Wave period, T_p	Gama, γ	Current speed, V_c
Case	11.4	7.1	12.1	2.2	0.8

Table 2 List of all selected KDPs

No.	Category	Discipline	KDPs	Symbol
1	A	Aero	Wind speed	V_w
2		Hydro	Current speed	V_c
3			Significant wave height	H_s
4			Peak period	T_p
5			Shape factor	γ
6	B	Aero	*Glauert* correction	a_c
7			Tower drag	$C^A_{d_{\text{Tower}}}$
8–13		Hydro	Added linear viscous damping matrix	C^H_{ld}
14–19			Added linear restoring matrix	C^H_r
20			Added static force (3, 3)	$F_{\text{static}(3,3)}$
21			Platform drag	$C^H_{d_{\text{Platform}}}$
22	C	Mooring	Wet density	M_{WD}
23			Axial stiffness	M_{AS}
24			Mooring drag	M_{Cd}
25–29		Structural dynamics	Polynomial flap first vibration modes	φ^1_x
30–34			Polynomial flap second vibration modes	φ^2_x
35–39			Polynomial edge first vibration modes	φ^1_y

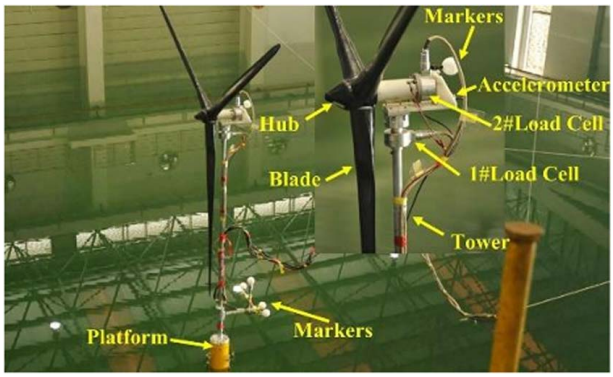

Fig. 9 Experimental model

Table 3 Boundary conditions of 39 KDPs in eight cases

No.	Fix	Small range	Large range	No range limit
BC1	B | C	A	–	–
BC2	C	A | B	–	–
BC3	–	A | B | C	–	–
BC4	–	B | C	A	–
BC5	–	C	A | B	–
BC6	–	–	A | B | C	–
BC7	–	–	B | C	A
BC8	–	–	C	A | B

5 SADA Analysis Results and Discussions

This section conducts an in-depth analysis of KDPs with the SADA method. The experimental data will be used to compare and discuss the optimization effects of different numbers of KDPs and different BCs in SADA.

5.1 The Impact of Key Disciplinary Parameter Numbers. This section will discuss the optimization effects of KDP numbers according to the analysis results and comparisons. The deep neural network is trained to optimize the correctness of its decision-making by storing the memory of each iteration. The trained SADA model uses the corresponding KDPs to calculate FOWT's dynamic response prediction. The result of percentage difference and amplitude changes are shown in Tables 4 and 5. In addition, Fig. 10 shows the percentage difference of some physical quantities. If the percentage difference is positive, the difference between the experiment and numerical simulation has decreased by SADA. It can be seen from Fig. 10 that the optimization results of group 3 (39) are better than group 1 and group 2.

This also means that the actual difference of the third group with the largest number 39 of KDPs is 70% lower than the traditional numerical calculation result that does not consider the change of KDPs. From the amplitude changes in Table 5, the fairlead tension and thrust are the most significant. Furthermore, these two physical quantities are one of the most critical parameters that affect the dynamic response of FOWTs. Figure 11 shows the time history of the surge motion. In the figure, the solid black line with large amplitude is the dynamic forecast without SADA. The black dotted line is the experimental result. The red line is the results of the third KDP group after SADA optimization.

The influence of KDPs can be discussed by the differences in different physical quantities during the process of SADA training. Figure 12 shows the percentage difference of four physical quantities in three groups in 100 training iterations. These four physical quantities are the surge motion of the platform, the pitch motion of the platform, the tension of the first fairlead (Fline1), and the axial thrust of the wind turbine. From Fig. 12, one key point can be obtained that the case with the largest KDPs number can reduce the oscillation of four physical quantities differences in the SADA training process. The percentage difference of four physical quantities in group 1 changes significantly in the environmental KDPs only. Especially in the first group, the relationship between thrust and pitch is negatively correlated. The oscillations of the four physical quantities in the second group are smaller than that in the first group because this group considers more KDP. The trend of pitch and thrust is similar, which can be observed in the third KDP group. Only environmental KDPs are considered, for example, simply increasing or decreasing wind speed, which cannot effectively improve the prediction of multiple physical quantities (due to the coupling effect). Therefore, when more KDPs are considered, the prediction of these physical quantities can be effectively improved.

5.2 The Impact of Boundary Conditions of Key Disciplinary Parameters. This section discusses the BCs of KDPs in the SADA method from two aspects:

- Difference reduction
- Iterative difference variation

Through the analysis of these aspects, the influence of KDPs of different BCs on the prediction difference of the dynamic response of FOWTs can be found. By analyzing the difference variation of each physical quantity in the SADA iteration process, the convergence effect of KDPs of different BCs can be evaluated. In addition, the statistical analysis of the difference variation of each physical quantity in the KDPs of different BCs can further determine the oscillating of physical quantities and the variation of the difference values. However, the initial BCs also need to be revised for some exceptional cases.

Table 4 Percentage difference of three groups (%)

	Surge	Sway	Heave	Roll	Pitch	Yaw	Fline1	Fline2	Fline3	Thrust
Group 1	1.231	7.944	1.143	−0.861	−1.612	−0.47	−0.148	0.021	0.036	−1.84
Group 2	0.028	7.879	−3.85	−0.347	0.718	−4.723	0.996	0.245	0.194	0.963
Group 3	3.604	27.439	−9.429	2.472	5.021	1.203	2.792	1.067	1.005	6.178

Table 5 Amplitude changes in three groups

	Surge (m)	Sway (m)	Heave (m)	Roll (deg)	Pitch (deg)	Yaw (deg)	Fline1 (kN)	Fline2 (kN)	Fline3 (kN)	Thrust (kN)
Group 1	0.114	0.006	−0.007	0.006	−0.105	0.006	−3.474	0.655	1.121	−17.112
Group 2	0.003	0.006	0.024	0.003	0.047	0.061	23.378	7.647	6.043	8.956
Group 3	0.333	0.022	0.058	−0.018	0.326	−0.015	65.533	33.301	31.306	57.455

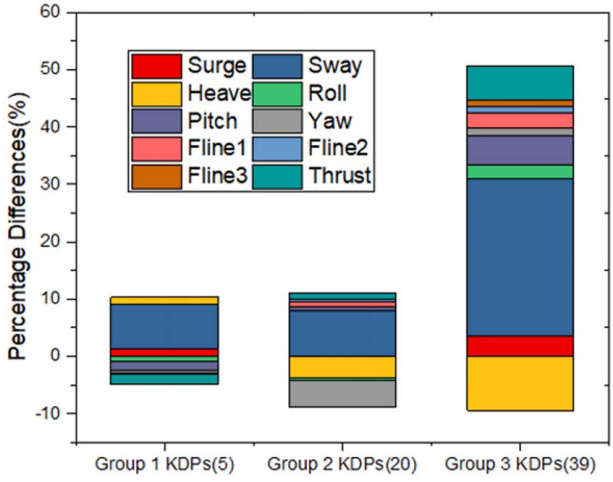

Fig. 10 The percentage difference of some physical quantities

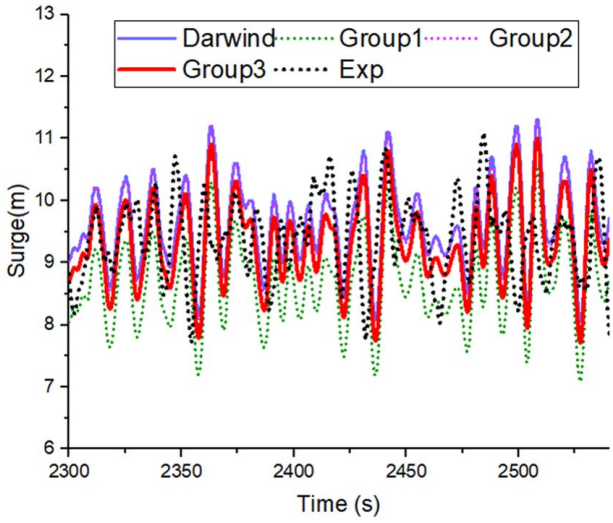

Fig. 11 The time history of the surge

5.2.1 Difference Reduction Analysis. This section uses the selected KDPs to analyze their impact on the FOWTs system under different BCs in the SADA method. The Gaussian distribution used for the weighting of KDPs is randomly weighted for each iteration. Figure 13 shows the percentage differences of four physical quantities (surge, pitch, fairlead tension force of the first fairlead, and wind turbine thrust) with eight BCs. And the corresponding amplitude changes of magnitudes are shown in Table 6.

The more considerable the positive difference variation, the better the SADA optimization effect, and the differences between original numerical and experimental have been significantly reduced. The optimization effect of the last five cases is much better than that of the first three (BC1, BC2, and BC3). The first three BCs are fixed or only allow for small changes of KDPs in each iteration. From the results of BC1, BC2, and BC3, the environmental KDPs play a very important role in optimizing surge, pitch, and thrust. In BC2 and BC3, the optimization of fairlead tension force has been improved significantly, especially when specific KDPs are added in BC3. Comparing BC3 with BC4, SADA balances the optimization of other physical quantities simultaneously by giving up the accuracy of part of the surge, which is also the intelligence of the SADA method. Although the difference changes were significant in BC4, BC5, and BC6, the amplitude of surge and pitch did not change significantly relative to thrust and

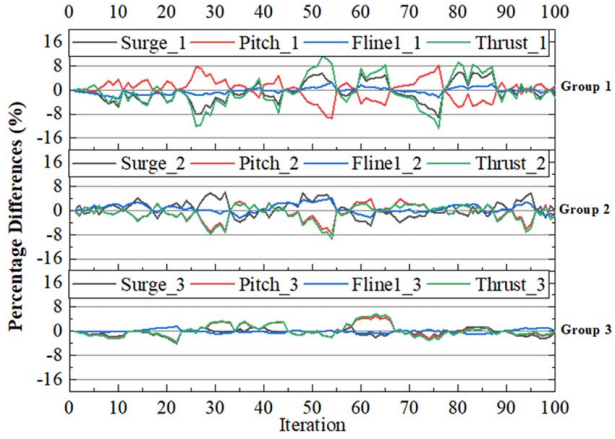

Fig. 12 The difference variation of three groups in iteration

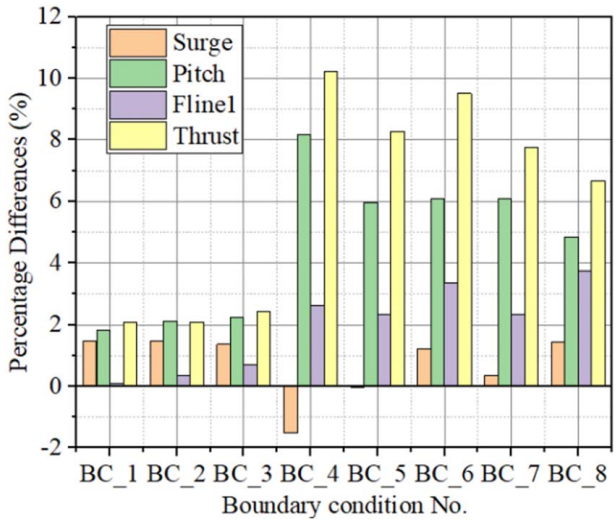

Fig. 13 The difference variation of eight BCs

Table 6 Amplitude changes of eight groups

KDP group	Surge (m)	Pitch (deg)	Fline1 (kN)	Thrust (kN)
BC1	0.137	0.119	1.901	19.384
BC2	0.135	0.137	8.262	19.347
BC3	0.127	0.146	16.853	22.780
BC4	−0.140	0.532	61.872	95.197
BC5	−0.004	0.388	54.830	76.930
BC6	0.114	0.394	79.217	88.572
BC7	0.033	0.396	54.877	72.277
BC8	0.134	0.314	88.136	62.078

fairlead tension, see Fig. 14. In contrast, the effect of the last two BCs has declined. For example, the thrust difference is reduced by about 6.5%, and the corresponding amplitude change is about 62 kN in BC8.

In general, as the combination of BCs of each group of KDPs changes, some summary can be roughly obtained:

(1) The environmental KDPs determine the relative maximum magnitude of the prediction accuracy.

The environmental KDPs have a vital influence on the forecast of the dynamic responses of the FOWTs system. Due to the measurement difference in the experiment or the simplification of the numerical model, larger BCs of the environmental KDPs are recommended. However, for

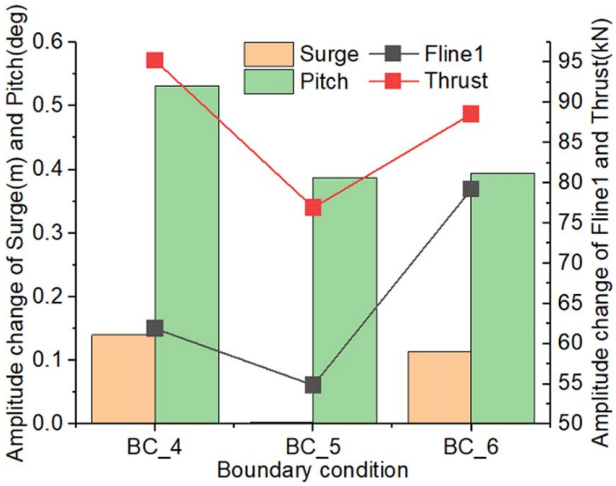

Fig. 14 The amplitude changes of three BCs

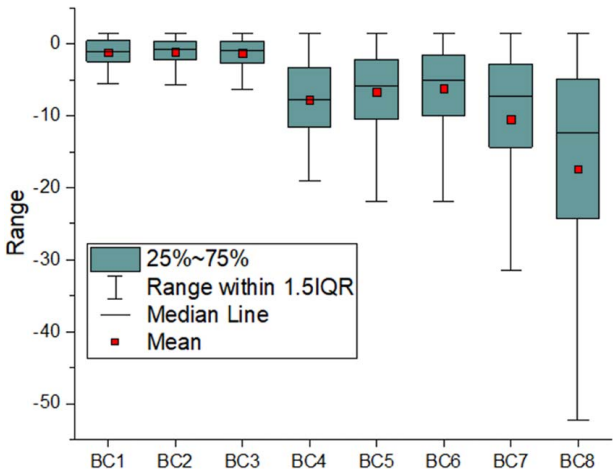

Fig. 15 Boxplot of surge in eight BCs

the forecast of some physical quantities, such as Fairlead tension force, it is not enough to only consider the environmental KDPs.

(2) KDPs with large BCs improve the prediction accuracy significantly.

KDPs with larger BCs can significantly improve the prediction accuracy of dynamic response prediction of FOWTs. In addition, SADA can intelligently balance the accuracy of each physical quantity by adjusting KDPs to avoid overfitting a particular physical quantity.

5.2.2 Statistical Analysis. This section will discuss the statistical results of percentage difference variation to analyze the oscillation relationship between different physical quantities and the BCs of KDPs can be found. The statistical results of different physical quantities under eight BCs are shown in Figs. 15–18.

In Fig. 15, the mean value of surge is the same in the first three BCs. Since the numerical results of surge without SADA optimization were originally predicted to have a percentage difference of 1.5%, the maximum values of the first three BCs were all around 1.5%. The mean values of the last five groups of BCs varied widely. However, the minimum value varies with the boundary conditions of the KDPs. Therefore, if the percentage of the physical quantities not optimized by SADA is small, the BCs with small boundaries are more reasonable. In Fig. 16, the mean of the percentage difference in pitch is the same among the first three BCs. However, its maximum value is limited by a small range of the

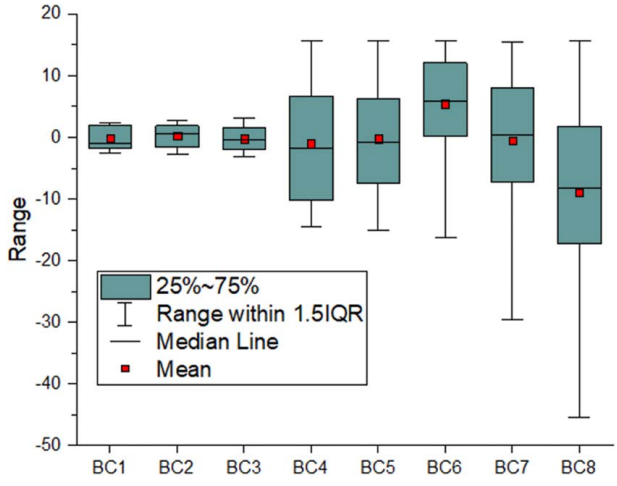

Fig. 16 Boxplot of pitch in eight BCs

BCs. In the last five BCs, the mean value of the mean of the percentage difference of pitch fluctuates significantly with the change of BCs of KDPs. The maximum value has reached about 15.65%, which is also the original percentage difference of pitch without SADA. Therefore, for such physical quantities, it may be more reasonable to give BCs a larger range.

In Fig. 17, the tension of the first fairlead is different from the changing trend of the first two physical quantities, and the mean value of the percentage difference in BCs is the most ideal in eight BCs. Although a larger BC of environmental KDPs can lead to a good percentage difference of Fline1, a reasonable combination of different BCs of the three sets of KDPs can achieve faster convergence and good results. For example, the combination of environmental KDPs with a larger range and the other two groups of KDPs with a small range can effectively obtain a good percentage difference of Fline1. In Fig. 18, The changing trend of the percentage difference of thrust among the eight BCs is similar to that of pitch in Fig. 16.

Based on the above analysis, it can be summarized that the oscillation of prediction accuracy is mainly caused by environmental KDPs, which play a decisive factor in this phenomenon. The other two types of KDPs may effectively reduce the oscillation of prediction accuracy based on specific conditions and physical quantities during the expansion of BCs.

5.3 Boundary Conditions Adjustment for the Specific Situation. This section adjusts BCs on the original basis for some specific situations. Through these adjustments, not only can the prediction accuracy be better but also good results can be obtained more efficiently.

The result without AI-based surge motion is already close to the experimental value, for example, the original percentage difference of surge between numerical simulation and experiment is 1.5% in Fig. 15. If the KDPs are slightly changed, the difference of surge will have a relatively large oscillation. In addition, even though the differences between the first six groups of BCs have risen, they oscillated within a small range. For KDPs without limiting BCs, the oscillation of the mean difference of surge is very significant. For a specific situation, when one or more dynamic response quantities of the FOWTs system already have a very high accuracy without AI-based, the BCs of the first six BCs may be more applicable for training, and they are fully capable of reducing the existing differences. For other physical quantities, the optimization of small BCs is minimal for pitch motion, see Fig. 16. The optimization effects of the eight BCs on the fairlead tension are similar. Therefore, a larger boundary condition based on KDPs seems more reasonable for fairlead tension, see Fig. 17. The small BC of

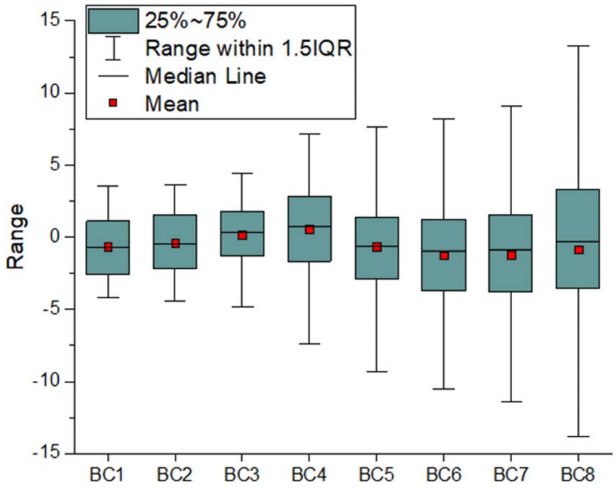

Fig. 17 Boxplot of Fline1 in eight BCs

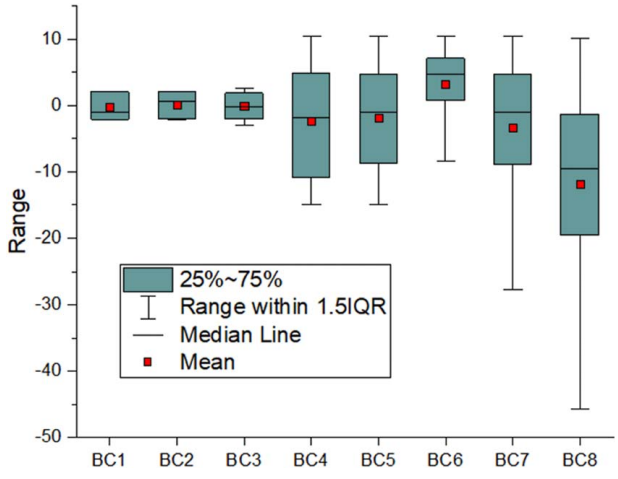

Fig. 18 Boxplot of thrust in eight BCs

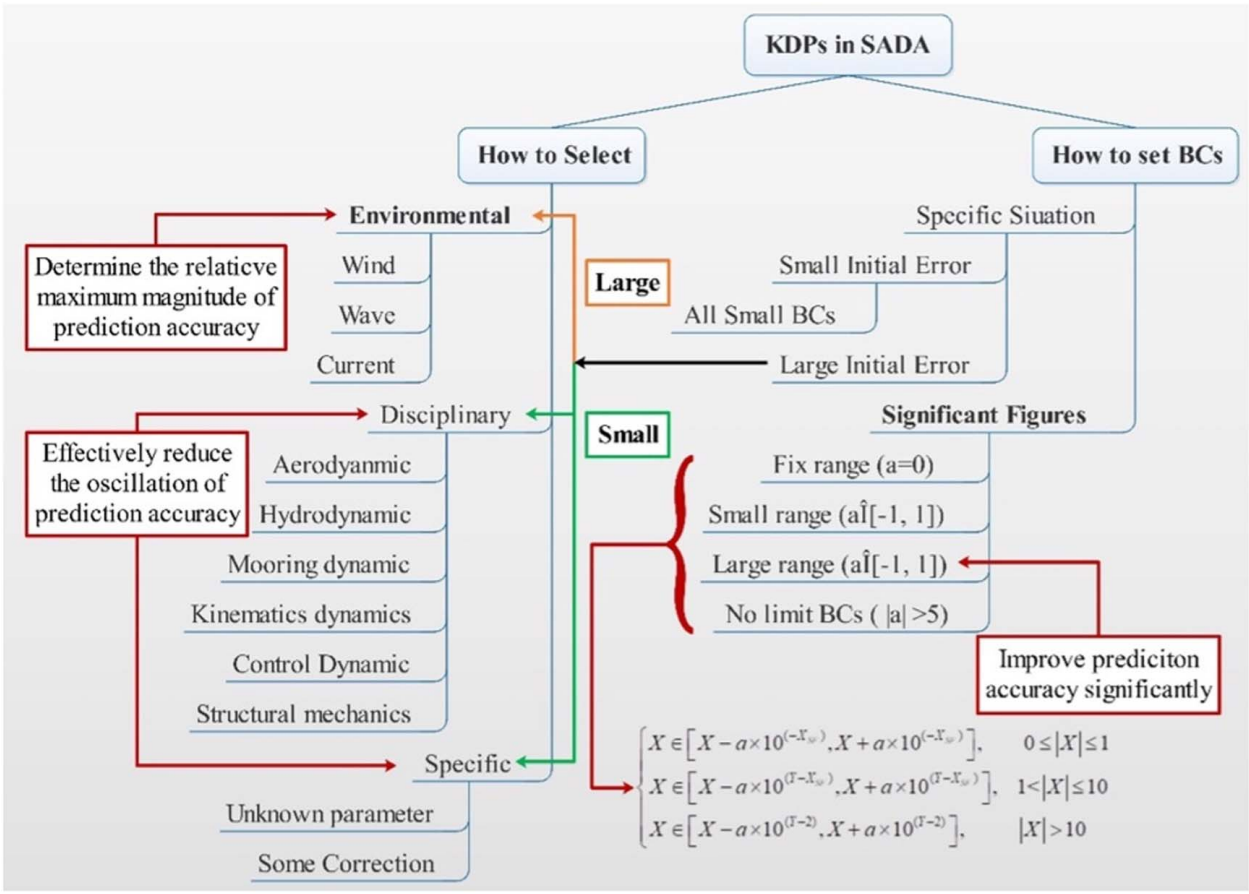

Fig. 19 The flowchart of KDPs in SADA

environmental KDPs only have limited optimization of the thrust force. The latter five groups of BCs can reduce the differences in thrust force by up to about 10%.

In general, for the physical quantities of different initial differences between numerical simulation and target data, the effects of each BCs are different, which puts forward higher requirements for the adjustment of BCs. Based on the above analysis, it can be summarized as the following points:

(1) The initial difference in target physical quantity is small

Due to the slight initial difference, selecting BCs with larger boundary conditions requires careful consideration. The significant difference oscillation may happen, affecting the prediction accuracy of other physical quantities due to the solid nonlinear coupling of the entire system. Therefore, it may be more appropriate to choose smaller BCs when the initial difference in target physical quantity is small.

(2) Significant initial difference of target physical quantity

It is inevitable to encounter relatively significant initial differences in specific physical quantities (for example, greater than 20%). It may be necessary to choose between small BCs (disciplinary and specific KDPs) and large BCs (environmental KDPs).

5.4 Summary. Finally, corresponding guidance methods and suggestions are given for KDPs. Comprehensive guidance on the application of KDPs in the SADA method is shown in Fig. 19 to summarize the analysis of the proposed KDPs concept, including how to select and how to set BCs. The specific decision process is as follows:

- Step 1: Choose the corresponding KDPs in the three categories.
- Step 2: Use the concept of significant figures to set the boundary conditions according to the specific values of each KDP.
- Step 3: Determine the allowable error magnitude of the numerical calculation result and the target data (can be experimental data or measured data).
- Step 4: Adjust the boundary conditions appropriately.

6 Conclusion

This paper analyses and discusses the selection and boundary conditions of KDPs involved in the field of FOWTs. Based on the determinism of physical phenomena, using AI technology to adjust these KDPs through self-learning intelligently is one of the critical technologies of the SADA method. In addition to a higher accurate numerical model, laws of KDPs are needed. It can be pointed out that a better optimization effect through the SADA method can be achieved with a greater number of KDPs, the environmental KDPs are one of the most significant factors affecting the dynamic response of the entire FOWTs system, and all KDPs need to cooperate with a relatively suitable boundary condition. Nevertheless, the correlation analysis of the mutual influence between different KDPs in the dynamic response prediction of the entire FOWTs system is ignored in this study, and it will be included in future work.

Acknowledgment

The authors would like to thank the support from the National Natural Science Foundation of China (Nos. 42176210 and 52201330), and the Oceanic 488 Interdisciplinary Program of Shanghai Jiao Tong University (Grant No. SL2021PT203).

Conflict of Interest

There are no conflicts of interest.

Data Availability Statement

The datasets generated and supporting the findings of this article are obtainable from the corresponding author upon reasonable request.

References

[1] Hannon, M., Topham, E., Dixon, J., McMillan, D., and Collu, M., 2019, *Offshore Wind, Ready to Float? Global and UK Trends in the Floating Offshore Wind Market*, University of Strathclyde, Glasgow.

[2] Jonkman, J., and Musial, W., 2010, "Offshore Code Comparison Collaboration (OC3) for IEA Wind Task 23 Offshore Wind Technology and Deployment," National Renewable Energy Lab. (NREL), Golden, CO.

[3] Robertson, A., Jonkman, J., Masciola, M., Song, H., Goupee, A., Coulling, A., and Luan, C., 2014, "Definition of the Semisubmersible Floating System for Phase II of OC4," http://purl.fdlp.gov/GPO/gpo43219

[4] Robertson, A. N., Wendt, F., Jonkman, J. M., Popko, W., Dagher, H., Gueydon, S., Qvist, J., et al., 2017, "OC5 Project Phase II: Validation of Global Loads of the DeepCwind Floating Semisubmersible Wind Turbine," Energy Procedia, **137**(Part of Special Issue: 14th Deep Sea Offshore Wind R&D Conference, EERA DeepWind'2017), pp. 38–57.

[5] Robertson, A. N., Gueydon, S., Bachynski, E., Wang, L., Jonkman, J., Alarcón, D., Amet, E., Beardsell, A., Bonnet, P., and Boudet, B., 2020, "OC6 Phase I: Investigating the Underprediction of Low-Frequency Hydrodynamic Loads and Responses of a Floating Wind Turbine," J. Phys. Conf. Series, **1618**, p. 032033.

[6] Popko, W., Robertson, A., Jonkman, J., Wendt, F., Thomas, P., Müller, K., Kretschmer, M., et al., 2021, "Validation of Numerical Models of the Offshore Wind Turbine From the Alpha Ventus Wind Farm Against Full-Scale Measurements Within OC5 Phase III," ASME J. Offshore Mech. Arct. Eng., **143**(1), p. 012002.

[7] Chen, P., Chen, J., and Hu, Z., 2020, "Review of Experimental-Numerical Methodologies and Challenges for Floating Offshore Wind Turbines," J. Mar. Sci. Appl., **19**(3), pp. 339–361.

[8] Assets, O. R. F. C. O., 2021, "Publications—Robot & Asset Self-Certification," https://orcahub.org/latest/publications/publications-robot-asset-self-certification

[9] Garnier, P., Viquerat, J., Rabault, J., Larcher, A., Kuhnle, A., and Hachem, E., 2021, "A Review on Deep Reinforcement Learning for Fluid Mechanics," Comput. Fluids, **225**, p. 104973.

[10] Garmier, P., Viquerat, J., Rabault, J., Larcher, A., Kuhnle, A., and Hachem, E., 2021, "A Review on Deep Reinforcement Learning for Fluid Mechanics," Computers & Fluids, **225**, p. 104973.

[11] Li, L., Gao, Z., and Yuan, Z.-M., 2019, "On the Sensitivity and Uncertainty of Wave Energy Conversion With an Artificial Neural-Network-Based Controller," Ocean Eng., **183**, pp. 282–293.

[12] Li, L., Gao, Y., Ning, D., and Yuan, Z., 2020, "Development of a Constraint Non-Causal Wave Energy Control Algorithm Based on Artificial Intelligence," Renew. Sustain. Energy Rev., **138**, p. 110519.

[13] Xie, Y., Zhao, X., and Luo, M., 2022, "An Active-Controlled Heaving Plate Breakwater Trained by an Intelligent Framework Based on Deep Reinforcement Learning," Ocean Eng., **244**, p. 110357.

[14] Li, G., and Shi, J. J. A. E., 2010, "On Comparing Three Artificial Neural Networks for Wind Speed Forecasting," Appl. Energy, **87**(7), pp. 2313–2320.

[15] Pelletier, F., Masson, C., and Tahan, A., 2016, "Wind Turbine Power Curve Modelling Using Artificial Neural Network," Renew. Energy, **89**, pp. 207–214.

[16] Li, S., 2003, "Wind Power Prediction Using Recurrent Multilayer Perceptron Neural Networks," 2003 IEEE Power Engineering Society General Meeting (IEEE Cat. No. 03CH37491), Toronto, ON, Canada, July 13–17, IEEE, pp. 2325–2330.

[17] Kusiak, A., Zheng, H., and Song, Z., 2009, "Wind Farm Power Prediction: A Data-Mining Approach," Wind Energy, **12**(3), pp. 275–293.

[18] Sun, H., Qiu, C., Lu, L., Gao, X., Chen, J., and Yang, H. J. A. E., 2020, "Wind Turbine Power Modelling and Optimization Using Artificial Neural Network With Wind Field Experimental Data," Appl. Energy, **280**, p. 115880.

[19] Stetco, A., Dinmohammadi, F., Zhao, X., Robu, V., Flynn, D., Barnes, M., Keane, J., and Nenadic, G., 2019, "Machine Learning Methods for Wind Turbine Condition Monitoring: A Review," Renew. Energy, **133**, pp. 620–635.

[20] Chen, P., Chen, J., and Hu, Z., 2021, "Software-in-the-Loop Combined Reinforcement Learning Method for Dynamic Response Analysis of FOWTs," Front. Mar. Sci., **7**, p. 1242.

[21] Chen, P., Song, L., Chen, J.-H., and Hu, Z., 2021, "Simulation Annealing Diagnosis Algorithm Method for Optimized Forecast of the Dynamic Response of Floating Offshore Wind Turbines," J. Hydrodyn., **33**(2), pp. 216–225.

[22] Chen, J., Hu, Z., Liu, G., and Wan, D., 2019, "Coupled Aero-Hydro-Servo-Elastic Methods for Floating Wind Turbines," Renew. Energy, **130**, pp. 139–153.

[23] Faltinsen, O., 1993, *Sea Loads on Ships and Offshore Structures*, Cambridge University Press, Cambridge.

[24] Hansen, M. O. L., 2015, *Aerodynamics of Wind Turbines*, Routledge, London.

[25] Duan, F., Hu, Z., and Niedzwecki, J., 2016, "Model Test Investigation of a Spar Floating Wind Turbine," Mar. Struct., **49**, pp. 76–96.